



# Greenhouse gas dynamics in tropical montane streams of Puerto Rico and the role of watershed lithology

Allison M. Herreid · Carla López Lloreda ·

Adam S. Wymore · Jody D. Potter ·

William H. McDowell

Received: 30 March 2022 / Accepted: 3 November 2022  
© The Author(s), under exclusive licence to Springer Nature Switzerland AG 2022

**Abstract** The major greenhouse gases in streams and rivers, carbon dioxide ( $\text{CO}_2$ ), methane ( $\text{CH}_4$ ), and nitrous oxide ( $\text{N}_2\text{O}$ ), can contribute significantly to regional greenhouse gas (GHG) budgets, and each appears to be responding to multiple drivers. Recent work suggests that tropical water bodies may be hot spots of GHG emissions due to high primary productivity in their watersheds, but tropical streams and rivers have historically been underrepresented in studies of GHG concentration and emissions. We use a five-year record of weekly water chemistry and dissolved gas data from eight tropical watersheds of varying lithology and redox conditions in the Luquillo Mountains of Puerto Rico to examine controls on GHG variability and estimate gas flux. Streams were frequently supersaturated in all three gases indicating

that streams in this tropical landscape are sources of GHGs to the atmosphere. Concentrations of  $\text{CO}_2$  and  $\text{N}_2\text{O}$  were associated with lateral inputs from the surrounding landscape, whereas  $\text{CH}_4$  concentrations correlated with in-stream oxygen availability and lithology. Our results underscore the importance of including tropical sites in global syntheses and budgets and the role of both in-stream biological and physical processes as well as landscape attributes that contribute to the export of gases to the fluvial network and atmosphere.

**Keywords** Greenhouse gas · Carbon dioxide · Methane · Nitrous oxide · Tropical · Stream

## Introduction

Streams and rivers are important sources of carbon dioxide ( $\text{CO}_2$ ; Cole et al. 2007; Drake et al. 2018), methane ( $\text{CH}_4$ ; Stanley et al. 2016), and nitrous oxide ( $\text{N}_2\text{O}$ ; Quick et al. 2019) to the atmosphere. Our current understanding of greenhouse gas (GHG) patterns, controls, and fluxes is driven primarily by studies coming from temperate and populated areas (e.g., Stanley et al. 2016), with an underrepresentation of Arctic and tropical zone latitudes (Lauerwald et al. 2015). Although there is a comparatively small number of studies on  $\text{CO}_2$  outgassing from tropical systems, a recent synthesis suggests a disproportionate contribution of  $\text{CO}_2$  from subtropical and equatorial

---

Responsible Editor: Jacques C. Finlay

---

**Supplementary Information** The online version contains supplementary material available at <https://doi.org/10.1007/s10533-022-00995-9>.

---

A. M. Herreid · C. L. Lloreda · A. S. Wymore ·  
J. D. Potter · W. H. McDowell  
Department of Natural Resources and the Environment,  
University of New Hampshire, 56 College Road, Durham,  
NH, USA  
e-mail: allison.herreid@unh.edu

*Present Address:*  
C. L. Lloreda  
Department of Biological Sciences, Virginia Polytechnic  
Institute and State University, Blacksburg, VA, USA

regions to global riverine fluxes (Lauerwald et al. 2015). It has yet to be determined if fluvial emissions of  $\text{CH}_4$  and  $\text{N}_2\text{O}$  from tropical regions are similarly important to global estimates. Our ability to accurately quantify GHG fluxes from tropical ecosystems is limited by a paucity of studies and uneven and spatiotemporally limited data coverage. Although a recent global synthesis included tropical  $\text{CH}_4$  emissions from 23 different studies, all were classified as ‘rivers’, suggesting that there is a gap in studies measuring GHGs in smaller streams in the tropics (Rosentreter et al. 2021). There is a need for direct, long-term measurements of GHGs from diverse tropical ecosystems to more accurately represent the role of tropical inland waters in global GHG fluxes.

Given the aseasonality, warm temperatures, hydrological extremes, and unique disturbance regimes that characterize much of the tropics, it is reasonable to expect varying patterns and controls on GHG concentrations compared with other biomes. The knowledge that we do have about controls on GHG concentrations and fluxes in tropical systems is dominated by studies from the Amazon basin that have primarily focused on  $\text{CO}_2$  dynamics (Lauerwald et al. 2015). Inflow of dissolved carbon and  $\text{CO}_2$  from groundwater, soil respiration, and wetlands have been identified as primary drivers of  $\text{CO}_2$  in many tropical and subtropical regions (Sadat-Noori et al. 2016; Duvert et al. 2019; Abril and Borges 2019; Schneider et al. 2020), corroborating the importance of landscape contributions to stream  $\text{CO}_2$  dynamics as also reported from temperate systems (Hotchkiss et al. 2015; Herreid et al. 2020). There is a growing number of studies measuring  $\text{CH}_4$  in tropical systems (e.g., Selvam et al. 2014; Teodoru et al. 2015; Bange et al. 2019; Rosentreter et al. 2021), however, considerably less emphasis has been placed on patterns of  $\text{CH}_4$  and  $\text{N}_2\text{O}$  concentrations in the tropics, particularly when considering factors driving the production of  $\text{CH}_4$  and  $\text{N}_2\text{O}$  (though see Borges et al. 2015; Upstill-Goddard et al. 2017). Spatial variability in  $\text{CH}_4$  and  $\text{N}_2\text{O}$  may be considerable in some tropical locations, especially those characterized by strong redox gradients (Liptzin et al. 2011; Liptzin and Silver 2015).

Few studies investigate controls and mechanisms driving variability in concentrations and fluxes of all three major GHGs ( $\text{CO}_2$ ,  $\text{CH}_4$ ,  $\text{N}_2\text{O}$ ) when measured together, which is essential for improving global models and developing a better understanding of

factors driving GHG dynamics across biomes. Here, we use a five-year record of weekly data from eight streams and rivers within the Luquillo Mountains in Puerto Rico to examine potential controlling mechanisms and provide flux estimates of  $\text{CO}_2$ ,  $\text{CH}_4$ , and  $\text{N}_2\text{O}$  in tropical montane watersheds with differing lithologies and forest types (McDowell et al. 2021). We hypothesize that the availability of dissolved organic carbon (DOC) will drive collective gas concentrations, given the need for an energy source for many gas-producing pathways. We hypothesize that  $\text{CO}_2$  will be tightly linked to in-stream dissolved oxygen ( $\text{O}_2$ ) concentrations due to the links between respiration and primary production. However, we expect this relationship to diverge from the theoretical 1:1 ratio given potential  $\text{CO}_2$  inputs from anaerobic respiration and external inputs from the surrounding landscape (Crawford et al. 2014). We expect  $\text{CH}_4$  to be related to conditions favorable for methanogenesis (i.e., low  $\text{O}_2$ , high DOC, small sediment size; Stanley et al. 2016), and  $\text{N}_2\text{O}$  to be related to the availability of dissolved nitrogen (nitrate, ammonium, total dissolved nitrogen) and  $\text{O}_2$  given the requirements of  $\text{N}_2\text{O}$ -producing pathways (Quick et al. 2019).

## Methods

### Site description

Study sites are located in the Luquillo Experimental Forest of northeastern Puerto Rico (Fig. 1; McDowell et al. 2021). Compared with flat, lowland tropical sites, our study region includes watersheds that drain mountainous, steep gradient tropical landscapes. The average air temperature in the Luquillo Mountains is above 20 °C with rainfall varying from 2500 to 4500 mm depending on elevation (McDowell et al. 2012; Murphy et al. 2017). The Luquillo Mountains vary in lithology, and streams and rivers that drain the mountain landscape reflect these differences in lithology (Wymore et al. 2017; Hynek et al. 2022). Our study sites (Table 1) are paired and include a larger mainstem river and a smaller tributary stream in each of the three dominant lithologies (volcanic-clastic, quartz diorite, and hornfels). Differences in lithology result in different weathering regimes, variable oxygen availability and contrasting stream channel attributes, with sand-filled channels typical in

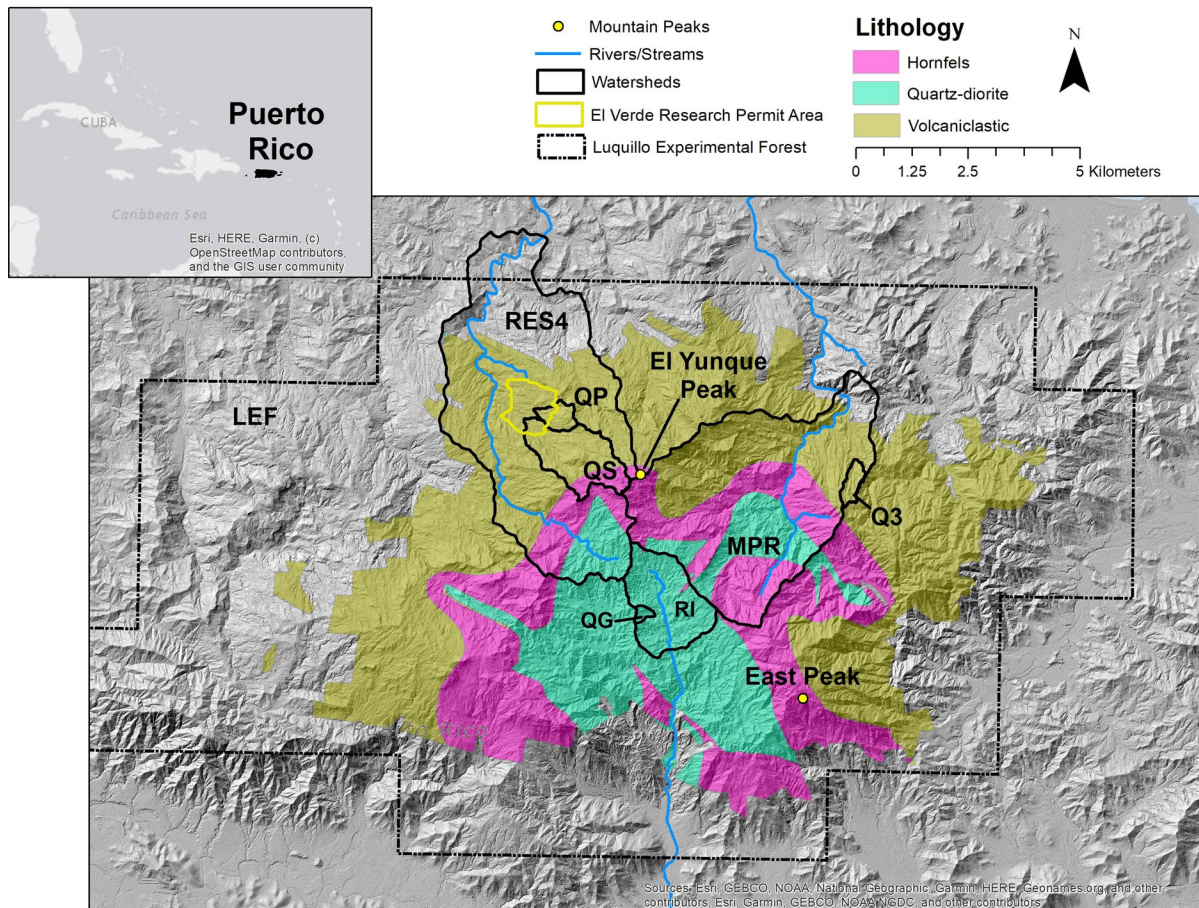


**Fig. 1** Map of the Luquillo Mountains and the Luquillo Experimental Forest in Puerto Rico. Watersheds are outlined in black, and colors denote major lithology types. RI: Río Icacos; QG: Quebrada Guabá; MPR: Mameyes at Puentे Roto; Q3: Bisley 3; RES4: Río Espíritu Santo; QS: Quebrada Sonadora; QP: Quebrada Prieta. QPA and QPB are located near the point labeled QP, with the two tributaries (QPA, QPB) sampled before the confluence. Map provided by Miguel Leon and used with permission

high-elevation watersheds underlain by quartz diorite, and large boulders in steeply sloped streams draining volcaniclastic and hornfels landscapes (Pike et al. 2010; McDowell et al. 2021).

#### Data collection

Our dataset includes weekly water chemistry and dissolved gas data collected between April 2015 and December 2019, resulting in a total of 965 observations across the eight sites. One water and one gas sample were collected at each stream during each sampling event. Water chemistry samples were collected in acid-washed syringes and filtered using pre-combusted glass fiber filters (0.7  $\mu\text{m}$ ; Whatman

GF/F) and stored on ice immediately following collection. Samples were frozen or refrigerated until the time of analysis. Dissolved oxygen, specific conductance, pH, and water temperature measurements were recorded at the time of sample collection using a YSI multiparameter probe (YSI ProDSS, Yellow Springs, OH). Dissolved gas samples were collected using acid-washed syringes equipped with three-way stopcocks. Syringes were rinsed and filled to 30 mL underwater after clearing air bubbles. Syringes were kept on ice and were equilibrated into a headspace of ultrapure helium and stored in evacuated vials within eight hours of collection.

Substrate particle size was characterized at three of the streams (QP, QS, and RI) based on the smallest

**Table 1** Characteristics of study watersheds: watershed area (Area km<sup>2</sup>); mean catchment slope (Slope, °); mean elevation at sampling location (Elevation, Meters Above Sea Level); Lithology: Volcaniclastic (% VC); Quaternary (% Q); Quartz

Watershed	Area (km <sup>2</sup> )	Slope (°)	Elevation (MASL)	Lithology				Vegetation			
				% VC	% Q	% QD	% Hf	% SP	% Co	% DP	% Tab
<b>MPR</b>	17.7	22.6	498	38.8	0.1	20.3	40.8	19	13	5	60
Q3	0.28	20.9	543	100.0	0.0	0.0	0.0	0	0	0	100
<b>RI</b>	3.3	14.6	686	0.0	0.0	99.4	0.6	20	78	2	0
QG	0.13	17.5	643	0.0	0.0	100.0	0.0	0	100	0	0
<b>QS</b>	2.6	17.4	740	66.1	0.0	0.0	33.9	32	53	7	8
<b>QP</b>	0.31	15.9	431	100.0	0.0	0.0	0.0	66	0	0	34
QPA	0.03	18.5	507	100.0	0.0	0.0	0.0	100	0	0	0
QPB	0.16	16.3	582	100.0	0.0	0.0	0.0	93	7	0	0

Organized where downstream river is bold faced and nested tributaries are indented

size opening that the substrate could pass through on a gravelometer. Ten transects were established roughly 10 m apart along a~100 m reach. At each transect, ten substrate readings were taken along the width of the stream. Median (d50) substrate size was determined from cumulative frequency distributions.

#### Water chemistry analysis

Surface water samples were analyzed for concentrations of ammonium ( $\text{NH}_4^+$ ), total dissolved nitrogen (TDN), dissolved organic carbon (DOC), soluble reactive phosphorus (SRP), silica ( $\text{SiO}_2$  (aq)), and major cations (magnesium ( $\text{Mg}^{2+}$ ), calcium ( $\text{Ca}^{2+}$ ), potassium ( $\text{K}^+$ ), and sodium ( $\text{Na}^+$ )) and anions (chloride ( $\text{Cl}^-$ ), nitrate ( $\text{NO}_3^-$ ), and sulfate ( $\text{SO}_4^{2-}$ )). Major cations and anions were measured using ion chromatography (Anions/Cations Dionex ICS-1000/1100).  $\text{NH}_4^+$ ,  $\text{SiO}_2$  (aq), and phosphate as SRP were analyzed using a Seal Analytical AQ2 or SmartChem 200 discrete automated colorimetric analyzer. Measures of  $\text{NH}_4^+$  and  $\text{NO}_3^-$  refer to N only and are reported as  $\text{NH}_4\text{-N}$  and  $\text{NO}_3\text{-N}$ . DOC and TDN were measured by high-temperature catalytic oxidation with a Shimadzu TOC-L with a TNM-1 nitrogen analyzer.

#### Dissolved gas analysis

Each syringe was filled with 30 mL of helium and samples were shaken for 5 min to equilibrate gases between water and headspace (Mulholland et al.

Diorite (% QD); and Hornsfel (% Hf); and Vegetation: Sierra Palm (% SP); Colorado (% Co); Dwarf Palm (% DP); and Tabonuco (% Tab)

2004). The headspace was then stored in 20 mL evacuated vials for subsequent analysis at the University of New Hampshire. Gas samples were analyzed using a Shimadzu GC-2014 gas chromatograph equipped with a thermal conductivity detector to detect  $\text{CO}_2$ , a flame ionization detector for  $\text{CH}_4$ , and an electron capture detector to detect  $\text{N}_2\text{O}$ . Gas concentrations are reported in  $\mu\text{M}$  and the percentage saturation of each gas concentration was determined following standard procedures (Audet et al. 2017; Herreid et al. 2020).

#### Gas flux calculations

Gas flux estimations for each gas at a subset of study streams (QP, QS, and RI) were estimated using the following equation:

$$F = k(C_w - C_{eq})$$

where  $k$  (gas transfer velocity) is multiplied by the difference between the dissolved gas concentration in the water ( $C_w$ ) and the gas concentration expected at equilibrium with the atmosphere ( $C_{eq}$ ) (Beaulieu et al. 2011; Raymond et al. 2012). Gas transfer velocities were estimated using two approaches. Field measurements of reaeration coefficients were conducted at each site and used to calculate  $k$ . Reaeration coefficients were determined in the field using argon (Ar) as a conservative gas tracer. Background samples were collected at several stations along the reach prior to

conducting an addition of Ar. Ar was co-injected into the stream with NaCl at a constant rate. Conductivity was measured at the furthest downstream station. After detecting that conductivity had reached plateau, we recorded measurements of specific conductance, stream temperature, and barometric pressure, and collected water samples for Ar:N<sub>2</sub> (triplicate) and water chemistry at stations along the stream reach. The NaCl data were used to calculate travel time and discharge. Stream width and mean depth were measured at each station and were used with discharge to calculate velocity. Reaeration coefficients were then calculated following standard methods (Supplementary Table 1; Wanninkhof et al. 1990; Raymond et al. 2012). Slope and velocity of each stream reach were also used to model  $k$  using Eq. 3 from Raymond et al. (2012). We considered using the framework from Ulseth et al. (2019) for determining  $k$ , but ultimately determined that not all of our streams fall into the steep, high-energy category that would be considered well-suited for this approach. Instantaneous discharge measurements used in flux calculations were obtained from gauging stations of the United States Geological Survey (QS: 50063440; RI: 5007500) and the University of Puerto Rico (QP). We did not collect ebullitive CH<sub>4</sub> samples and thus our flux estimates represent diffusive CH<sub>4</sub> flux only.

#### Statistical analyses

Data were normalized using logarithmic transformations if they failed Shapiro–Wilk tests for assumptions of normality or exhibited high levels of skewness and kurtosis. Boxplots in combination with analysis of variance (ANOVA) and means separation were used to identify differences among sites and lithologies for each gas. We assessed bivariate relationships between dissolved gas concentrations and metrics of stream chemistry and environmental parameters using linear regression analysis. We present the relationship between dissolved CO<sub>2</sub> and O<sub>2</sub> as excess CO<sub>2</sub> and O<sub>2</sub>. Excess was calculated as the difference between measured CO<sub>2</sub> or O<sub>2</sub> concentrations and equilibrium concentrations expected if the stream water was in equilibrium with the atmosphere (i.e., 100% saturation). Thus, positive values indicate periods of supersaturation and negative values indicate depletion or undersaturation. If aerobic metabolism accounts for the majority of measured

CO<sub>2</sub> concentrations, data should largely fall on a 1:1 line (with a  $-1$  slope), but anaerobic respiration and large terrestrial inputs of CO<sub>2</sub> often cause this relationship to change (Crawford et al. 2014; Herreid et al. 2020). All statistical analyses were performed using R version 4.0.5 (R Core Team 2021) with an  $\alpha < 0.05$  being the significance threshold for all analyses.

## Results

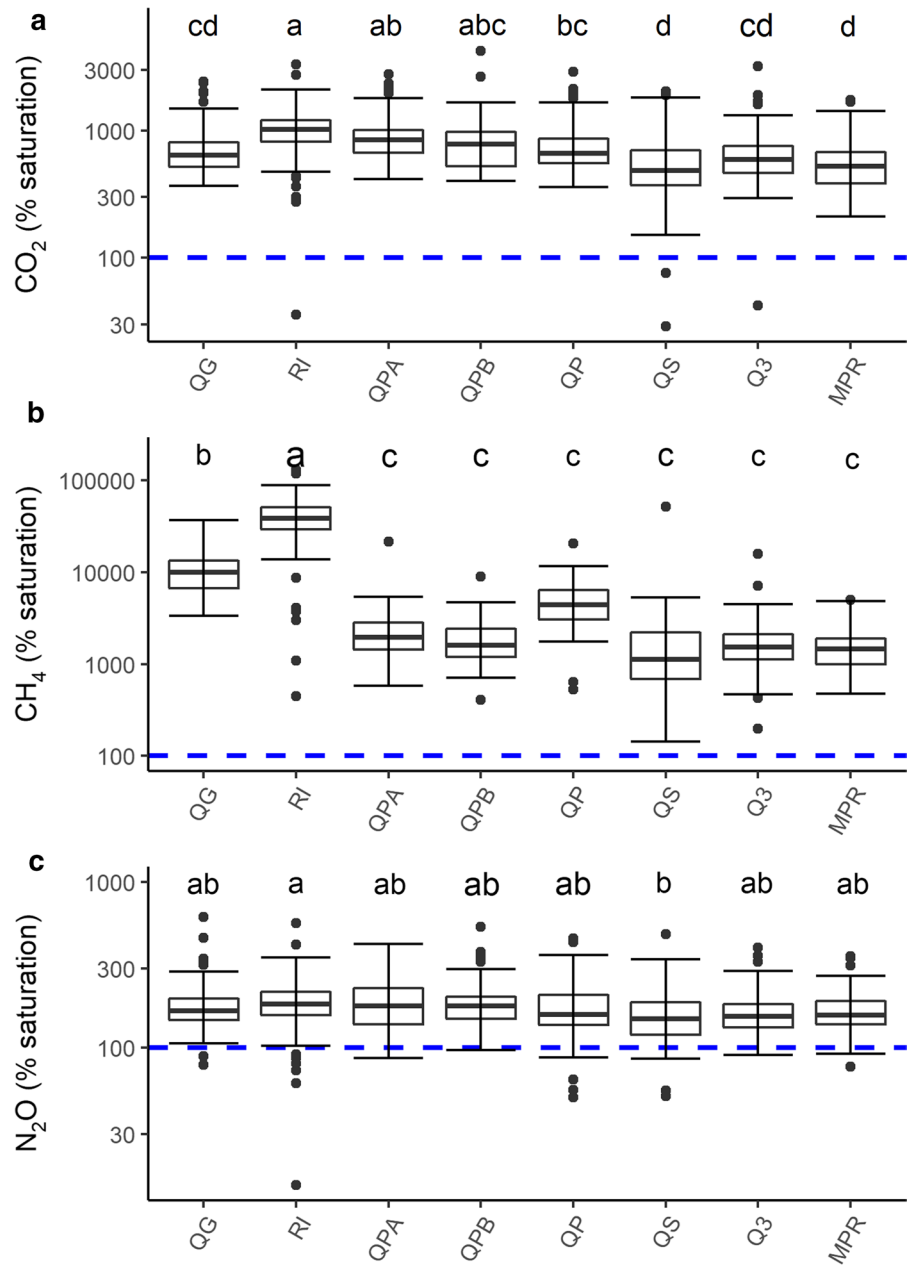
### Water chemistry and dissolved gases

Average concentrations of NO<sub>3</sub><sup>-</sup> ranged from 0.09 to 0.29 mg N L<sup>-1</sup> across sites and mean DOC concentrations were between 1.01 and 1.88 mg C L<sup>-1</sup> (Supplementary Table 2). Mean concentrations of other measured water chemistry analytes by site can be found in the supplemental material. Dissolved CO<sub>2</sub> concentrations ranged from 3.4 to 487  $\mu$ M (mean = 90  $\mu$ M) across all sites over the length of the dataset. Streams were almost always supersaturated in CO<sub>2</sub> (mean = 791% saturation) and exhibited minimal spatial variability among sites and between mainstem-tributary pairings (Fig. 2a; Table 1). Dissolved CH<sub>4</sub> concentrations ranged from  $3.5 \times 10^{-3}$  to 3.0  $\mu$ M (mean = 0.22  $\mu$ M) and varied among sites (Fig. 2b). The two watersheds primarily underlain by quartz diorite, RI and QG, had significantly higher CH<sub>4</sub> (% saturation) than all other sites ( $p < 0.0001$ ), with QG being significantly lower than RI ( $p < 0.0001$ ). All sites showed consistent supersaturation in CH<sub>4</sub> (mean = 9.164% saturation). Streams were generally supersaturated in N<sub>2</sub>O (mean = 181% saturation) and did not vary greatly among sites (Fig. 2c). Concentrations of dissolved N<sub>2</sub>O ranged from 1.1 to 46 nM (mean = 13 nM) across sites.

### Substrate particle size

Median particle size varied among sites and lithologies (Supplementary Table 3). Substrate at RI, underlain by quartz diorite, is predominantly sand (77%) with a d<sub>50</sub> of 1.65 mm. QP had a d<sub>50</sub> of 18.70 mm, and median particle size at QS was 160 mm.

**Fig. 2** Boxplot panels representing percent saturation for  $\text{CO}_2$  (a),  $\text{CH}_4$  (b), and  $\text{N}_2\text{O}$  (c) across the sampling period at 8 sites ( $n=747$ ). Sites are organized by nested watershed (see Table 1). Letters indicate statistically significant differences for between site comparisons. Data that fall above the dashed blue line at 100% indicate periods of supersaturation. Note that the y-axis of each panel is presented in log scale



#### Fluxes of GHGs

Fluxes calculated from modeled  $k$  were higher than those using measured  $k$  for RI and QP and lower for QS (Table 2). How and whether fluxes varied significantly among sites was dependent on if fluxes were calculated from modeled or measured  $k$  (see significance groupings in Table 2). Across

the three streams, mean  $\text{CO}_2$  flux calculated from measured  $k$  was  $1.84 \text{ mol m}^{-2} \text{ d}^{-1}$ , mean diffusive  $\text{CH}_4$  flux was  $1.79 \text{ mmol m}^{-2} \text{ d}^{-1}$ , and mean  $\text{N}_2\text{O}$  flux was  $194 \text{ } \mu\text{mol m}^{-2} \text{ d}^{-1}$ . On average, fluxes using modeled  $k$  were higher: mean  $\text{CO}_2$  flux was  $4.27 \text{ mol m}^{-2} \text{ d}^{-1}$ , mean diffusive  $\text{CH}_4$  flux was  $30.03 \text{ mmol m}^{-2} \text{ d}^{-1}$ , and mean  $\text{N}_2\text{O}$  flux across sites was  $307 \text{ } \mu\text{mol m}^{-2} \text{ d}^{-1}$ .

**Table 2** Mean gas transfer velocity ( $k$ ,  $\text{m d}^{-1}$ ), and fluxes of  $\text{CO}_2$  ( $\text{mol m}^{-2} \text{d}^{-1}$ ),  $\text{CH}_4$  ( $\text{mmol m}^{-2} \text{d}^{-1}$ ), and  $\text{N}_2\text{O}$  ( $\mu\text{mol m}^{-2} \text{d}^{-1}$ ) calculated using measured and modeled values for gas transfer velocity for each site.

QS	QP		RI		Mean flux	
	Measured	Modeled*	Measured	Modeled*	Measured	Modeled*
$k$	87.4 (104.8)	22.0 (12.3)	6.5 (10.6)	14.4 (18.3)	2.8 (5.0)	78.5 (39.5)
$\text{CO}_2$ flux	4.76 (6.16) <sup>a</sup>	1.25 (0.96) <sup>b</sup>	0.56 (1.11) <sup>b</sup>	1.25 (1.97) <sup>b</sup>	0.16 (0.27) <sup>b</sup>	9.43 (6.01) <sup>a</sup>
$\text{CH}_4$ flux	3.22 (4.71) <sup>a</sup>	0.94 (1.87) <sup>b</sup>	0.67 (1.01) <sup>b</sup>	1.59 (1.76) <sup>b</sup>	1.35 (1.87) <sup>b</sup>	79.1 (50.2) <sup>a</sup>
$\text{N}_2\text{O}$ flux	509 (1,272) <sup>a</sup>	118 (190) <sup>b</sup>	59.0 (248.6) <sup>b</sup>	122.6 (437.0) <sup>b</sup>	10.7 (25.5) <sup>b</sup>	627 (707) <sup>a</sup>

Standard deviation in parentheses

\*Modeled using Eq. 3 from Raymond et al. (2012)

Superscripts indicate significant differences between streams ( $p < 0.05$ )

## Drivers of GHGs

We found that lithology plays a strong role in regulating the relative magnitude of gases, particularly for  $\text{CH}_4$ . Methane (as % saturation) was significantly higher and more variable in the quartz diorite sites than in the volcaniclastic or mixed lithologies (Fig. 3). Carbon dioxide varied significantly among lithologies with quartz diorite sites being the highest, and volcaniclastic sites higher than mixed sites (Fig. 3). Nitrous oxide was more uniform across lithologies, with quartz diorite sites only being significantly higher than the sites with mixed lithologies (Fig. 3). We found no relationships between DOC and any of the three gases.

Contrary to our hypothesis, the negative relationship between excess  $\text{CO}_2$  and excess  $\text{O}_2$  was weak ( $r^2 = 0.07$ ,  $p < 0.0001$ , Fig. 4). Carbon dioxide was generally supersaturated while  $\text{O}_2$  was generally depleted, except at MPR (mixed lithology) where  $\text{O}_2$  was frequently above 100% saturation. The majority of data points fall to the right of the theoretical 1:1 line and excess  $\text{CO}_2$  spanned a much larger range ( $-10$  to  $475 \text{ mmol m}^{-3}$ ) than  $\text{O}_2$  ( $-60.2$  to  $16.5 \text{ mmol m}^{-3}$ ).

Simple linear regression analysis revealed a significant negative relationship between dissolved  $\text{CH}_4$  and oxygen concentrations ( $r^2 = 0.48$ ,  $p < 0.0001$ , Fig. 5). Methane concentrations did not correlate with any cations or anions. Similarly, and in contrast to our hypothesis, we found no relationships between  $\text{N}_2\text{O}$  and  $\text{NO}_3^-$ ,  $\text{NH}_4^+$ , TDN, dissolved  $\text{O}_2$  or any other measured water chemistry analyte.

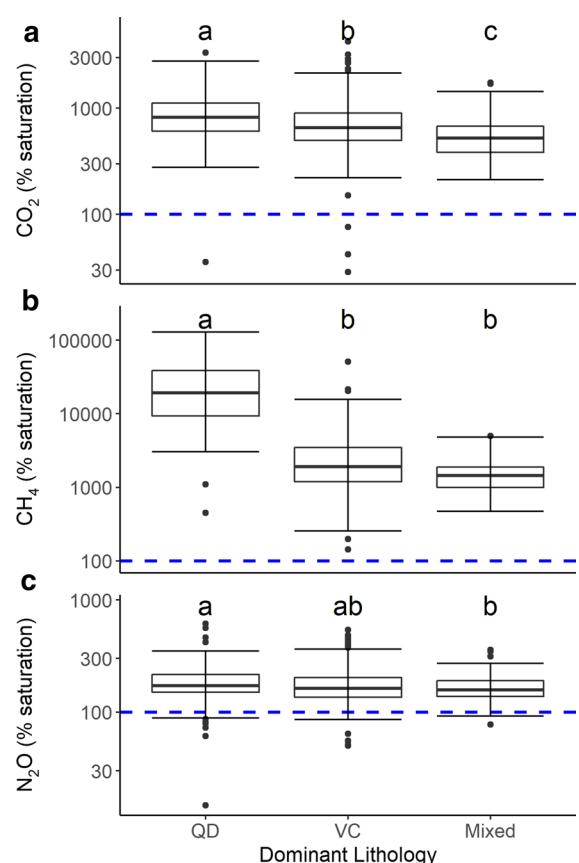


**Fig. 3** Boxplot representing differences between  $\text{CO}_2$  (a),  $\text{CH}_4$  (b) and  $\text{N}_2\text{O}$  (c) across the dominant lithology types (QD=Quartz Diorite, VC=Volcaniclastic). Letters indicate statistically significant differences ( $n=747$ )

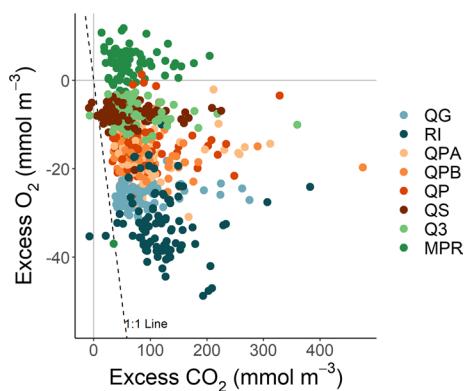


**Fig. 4** Relationship between excess  $\text{CO}_2$  and  $\text{O}_2$  ( $n=662$ ). Excess was calculated as the difference between measured and expected equilibrium concentrations (100% saturation). The dashed 1:1 line represents the theoretical relationship under the assumption that aerobic metabolism accounts for the majority of measured  $\text{CO}_2$  concentrations

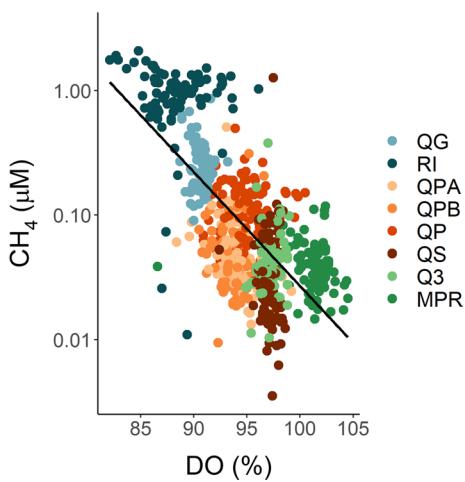


**Fig. 5** Linear regression between dissolved  $\text{CH}_4$  and oxygen across all sites ( $r^2=0.48$ ,  $p<0.0001$ ,  $n=685$ ). Note that the y-axis is presented on a log scale

## Discussion

Lithology and landscape contributions appear to drive GHG dynamics in watersheds within the Luquillo Mountains. Methane concentrations are largely a result of in-stream production, inferred from the negative relationship with dissolved  $\text{O}_2$  as well as the differences between sediment size (Pike et al. 2010, Supplementary Table 3) and redox status (Liptzin and Silver 2015) among lithologies. Concentrations

of  $\text{CO}_2$  and  $\text{N}_2\text{O}$ , in contrast, showed little variation with stream chemistry or other characteristics of our study streams, suggesting that lateral inputs from the terrestrial landscape may contribute to the variability in stream  $\text{CO}_2$  and  $\text{N}_2\text{O}$  concentrations. Production of  $\text{CO}_2$  through anaerobic respiration pathways may also contribute to  $\text{CO}_2$  variability and deviation from the theoretical 1:1 relationship with dissolved  $\text{O}_2$  (Fig. 4). Variability in mechanisms driving GHG dynamics, in our study and others, suggests different controls and patterns of GHGs in fluvial ecosystems globally. Our flux estimates, along with saturation calculations, suggest that streams and rivers in the Luquillo Mountains are generally sources of  $\text{CO}_2$ ,  $\text{CH}_4$ , and  $\text{N}_2\text{O}$  to the atmosphere. For all but one pair ( $\text{CO}_2$  and  $\text{CH}_4$  in QG and RI) in our nested watershed sampling design, the smaller tributary stream was just as supersaturated in all three gases as the larger mainstem river. This suggests that headwater and low-order streams may be disproportionate contributors of GHGs relative to larger rivers. The magnitude of the fluxes from this study in comparison with previous studies indicates that tropical inland waters may be important on the global scale for all three gases, not only  $\text{CO}_2$  (Laurerwald et al. 2015).

## Drivers of greenhouse gases

Stream water  $\text{CO}_2$  and  $\text{N}_2\text{O}$  concentrations in the Luquillo Mountains are likely a result of lateral inputs from the terrestrial landscape. Contrary to our hypothesis, we did not observe relationships between any of the greenhouse gases and DOC concentrations. It is possible that although the availability of DOC is important for gas production, we were not able to detect relationships in these low-DOC streams where consumption of labile DOC is rapid (Rodríguez-Cardona et al. 2021). We found no relationship between  $\text{N}_2\text{O}$  and  $\text{NO}_3^-$ , TDN, or  $\text{NH}_4^+$  even though  $\text{N}_2\text{O}$  concentrations are generally tightly linked to dissolved N and  $\text{O}_2$  availability (Burgin and Hamilton 2007; Quick et al. 2019) and relationships between  $\text{N}_2\text{O}$  and  $\text{NO}_3^-$  have been observed in riparian groundwater at one of our sites (RI; McDowell et al. 1992). However, our finding that  $\text{N}_2\text{O}$  is unrelated to concentrations of dissolved N is consistent with other tropical rivers (Borges et al. 2015; Bange et al. 2019) and suggests that production of  $\text{N}_2\text{O}$  is occurring in riparian zones due to the strong redox gradients and

**Table 3** Comparisons of ranges of excess CO<sub>2</sub> and O<sub>2</sub> from other studies. Means reported if available

Study	Biome	O <sub>2</sub> excess range	CO <sub>2</sub> excess range
This study	Tropical	−60.2 to 16.5 (mean = −14.5)	−10.0 to 475 (mean = 80.0)
Crawford et al. (2014) <sup>a</sup>	Temperate	−200 to 25	90 to 325
Herreid et al. (2020)	Temperate	−256.4 to 37.0 (mean = −53.6)	18–635 (mean = 151)
Rocher-Ros et al. (2019) <sup>a</sup>	Arctic	−90 to 5	−5 to 175

<sup>a</sup>Ranges were not reported and thus range listed represents estimates from figures

greater availability of NO<sub>3</sub><sup>−</sup> (McDowell et al. 1992). There is also evidence from a previous study in our study region (Potter et al. 2010) that denitrification proceeds to the most reduced end-product (N<sub>2</sub> over N<sub>2</sub>O) more often in streams than in soils and that the relationship between total denitrification (mostly N<sub>2</sub>) and aquatic N concentrations was strong. Studies assessing linkages between gas emissions from tropical forest soils and headwater streams found similar emissions of N<sub>2</sub>O from both soils and streams, underscoring the potential landscape connection for N<sub>2</sub>O dynamics in tropical systems (Potter et al. 2010; Barthel et al. 2022).

We also expected to see a negative relationship between dissolved O<sub>2</sub> and CO<sub>2</sub> due to the tradeoff between primary production and respiration, as has been identified in several studies (e.g., Crawford et al. 2014; Rocher-Ros et al. 2019; Herreid et al. 2020). The 1:1 line in Fig. 4 denotes this expected relationship under the assumption that aerobic metabolism produces the measured stream CO<sub>2</sub> concentrations. The majority of our data fall to the right of the 1:1 line, suggesting that other sources of CO<sub>2</sub> (i.e., anaerobic respiration, methane oxidation, or external inputs) contribute to the stream gas balance, consistent with other studies (e.g., Crawford et al. 2014; Herreid et al. 2020). In contrast to these other studies, and to sites globally, our range of dissolved O<sub>2</sub> is very narrow (Table 3) due to the high reaeration coefficients of these steep montane streams. This likely contributes to the lack of a significant relationship between CO<sub>2</sub> and O<sub>2</sub> at our sites.

In contrast to our results for N<sub>2</sub>O and CO<sub>2</sub>, we found that CH<sub>4</sub> concentrations were predictable by dissolved O<sub>2</sub> and varied with lithology (Figs. 3, 5) suggesting both biological and physical in-stream controls on CH<sub>4</sub> production. Higher concentrations of CH<sub>4</sub> are typically observed when O<sub>2</sub> becomes depleted due to the more reduced environment

required for methanogenesis (Stanley et al. 2016). Sites underlain by quartz diorite had significantly higher CH<sub>4</sub> than sites in the volcaniclastic or mixed lithology watersheds (Fig. 3). We attribute this control to differences in streambed characteristics as well as differing soil conditions between lithologies. Particle sizes are remarkably different between lithologies, with volcaniclastic watersheds containing larger particles with a more uniform size distribution (Phillips and Jerolmack 2016) and quartz diorite watersheds containing smaller particles that are often sand-dominated yet more heterogeneous (Pike et al. 2010, Supplementary Table 3). Providing both a source of organic matter and an anoxic environment, sediment deposition as well as the depth and supply of fine sediments have been shown to be important drivers of methanogenesis (Stanley et al. 2016; Bodmer et al. 2020; Herreid et al. 2020). The heterogeneity of quartz diorite stream beds may also drive the greater variability in CH<sub>4</sub> in these watersheds, as has been observed in water chemistry in previous studies (Wymore et al. 2019). This internal control of CH<sub>4</sub> production is consistent with another study in the tropics which found decoupling of aquatic CH<sub>4</sub> production from the terrestrial landscape and suggested the importance of production within benthic sediments or riparian zones (Barthel et al. 2022). Although the controls we discuss are related to CH<sub>4</sub> production, CH<sub>4</sub> oxidation may also be playing a role in the patterns we observed; however, our study was not designed to quantify the role of these two processes.

Concentrations and fluxes of greenhouse gases in a global context

Nitrous oxide concentrations in the Luquillo Mountains [1.1–46 nM (15–563% sat), mean = 13 nM (181% sat)] fall within the range of those reported

from other tropical and subtropical streams and rivers in sub-Saharan Africa (0.2–85.4 nM, mean = 9.2 nM, Borges et al. 2015; Upstill-Goddard et al. 2017; Marwick et al. 2018), southeast Asia (2.0–41.4 nM, Bange et al. 2019), and Australia (115–1430% sat, Andrews et al. 2021). Fluxes of  $\text{N}_2\text{O}$ , however, are much higher in the Luquillo Mountains relative to other tropical locations. Mean  $\text{N}_2\text{O}$  flux, as calculated from measured  $k$ , across the three streams was  $194 \mu\text{mol m}^{-2} \text{d}^{-1}$  whereas African streams and rivers ranged from 1 to  $67 \mu\text{mol m}^{-2} \text{d}^{-1}$  (Upstill-Goddard et al. 2017) and  $2–16 \mu\text{mol m}^{-2} \text{d}^{-1}$  (Borges et al. 2015), and average fluxes reported from southeast Asia and subtropical Australia were  $\sim 25 \mu\text{mol m}^{-2} \text{d}^{-1}$  (Bange et al. 2019) and  $4.01 \pm 5.98 \mu\text{mol m}^{-2} \text{d}^{-1}$  (Andrews et al. 2021), respectively. Soued et al. (2016) estimated average  $\text{N}_2\text{O}$  flux from high latitudes ( $> 54^\circ$ ) as  $1.7 \mu\text{mol m}^{-2} \text{d}^{-1}$ ,  $129 \mu\text{mol m}^{-2} \text{d}^{-1}$  from temperate streams and rivers ( $n=133$ ) and average tropical emissions of  $\text{N}_2\text{O}$  as  $60.8 \mu\text{mol m}^{-2} \text{d}^{-1}$  ( $n=15$ ). Thus, our sites have emissions of  $\text{N}_2\text{O}$  that are higher than typical for tropical systems and are comparable to temperate streams. Contextualizing our  $\text{N}_2\text{O}$  concentrations and fluxes at both a tropical and global scale remains difficult due to the paucity of measurements.

Dissolved  $\text{CH}_4$  concentrations from our study sites [0.006–3.03  $\mu\text{M}$  (144–128,767% sat), mean =  $0.22 \mu\text{M}$  (9.172% sat)] fall on the lower end of the global range [0–386  $\mu\text{M}$ , mean =  $1.35 \mu\text{M}$ ; Stanley et al. (2016)]. Compared to other tropical studies, our  $\text{CH}_4$  concentrations are comparable to those in Australia (0.19–62.13  $\mu\text{M}$ , Atkins et al. 2017; 428–9450% sat, Andrews et al. 2021) and fall within the range and are often higher than streams and rivers in the Amazon basin (0.02–0.5  $\mu\text{M}$ , Sawakuchi et al. 2014) and in Asia (0.0025–1.37  $\mu\text{M}$ , Bange et al. 2019). Fluxes of dissolved  $\text{CH}_4$  in our study using measured  $k$  ranged from  $-0.05$  to  $24.71 \text{ mmol m}^{-2} \text{d}^{-1}$  (mean =  $1.79 \text{ mmol m}^{-2} \text{d}^{-1}$ ). In comparison with other tropical systems, our fluxes are higher than those of streams in rivers in Australia ( $0.04 \text{ mmol m}^{-2} \text{d}^{-1}$ , Andrews et al. 2021), lower than those in Costa Rica (4.75 and  $5.96 \text{ mmol m}^{-2} \text{d}^{-1}$ , Oviedo-Vargas et al. 2015) and fall within the range of fluxes from the Amazon basin ( $0.01$ – $40.30 \text{ mmol m}^{-2} \text{d}^{-1}$ , Sawakuchi et al. 2014). Globally, fluxes from the Luquillo streams fall within the range reported by Stanley et al. (2016) ( $< 1$ – $40.49 \text{ mmol m}^{-2} \text{d}^{-1}$ ) but on average are lower than the global mean ( $4.23 \text{ mmol m}^{-2} \text{d}^{-1}$ ). It is

important to note that our  $\text{CH}_4$  fluxes only represent diffusive emissions. Ebullitive  $\text{CH}_4$  fluxes can be substantial and often higher than diffusive fluxes (e.g., Zheng et al. 2022), and thus our flux estimates are a conservative estimate of total  $\text{CH}_4$  flux.

Concentrations of  $\text{CO}_2$  in the Luquillo Mountains [3.4–487  $\mu\text{M}$  (29–4238% sat), mean =  $90 \mu\text{M}$  (791% sat)] are lower than the average reported for two streams in Costa Rica (mean =  $580 \mu\text{M}$ , Oviedo-Vargas et al. 2015) and within the range reported for Australian streams (520–1640% sat, Andrews et al. 2021). Mean  $\text{CO}_2$  flux from our streams ( $1.84 \text{ mol m}^{-2} \text{d}^{-1}$ ) was higher than both the global average reported by Lauerwald et al. (2015) for streams and rivers ( $0.46 \text{ mol C m}^{-2} \text{d}^{-1}$ ) as well as for small tropical streams ( $0.65 \text{ mol C m}^{-2} \text{d}^{-1}$ ). However, there are more recent tropical studies reporting higher fluxes (e.g.,  $74 \text{ mol m}^{-2} \text{d}^{-1}$ , Andrews et al. 2021).

Differences between fluxes observed in Luquillo streams and other tropical sites could be due to differences in precipitation, topography, and the well-documented role that lithology plays across this mountainous landscape. The steep topography alone results in larger reaeration values than would be observed in flatter tropical landscapes, which could be a reason why we see much higher fluxes of  $\text{N}_2\text{O}$  even when dissolved concentrations are comparable to other tropical sites. The relatively consistent precipitation patterns in Puerto Rico (McDowell et al. 2012), compared with tropical regions having distinct wet/dry seasons, along with the proposed riparian production of  $\text{N}_2\text{O}$  and  $\text{CO}_2$ , may also explain some of the variability between Luquillo streams and other tropical streams.

#### Flux estimates using measured versus modeled $k$

Many studies use a modelling approach (e.g., equations in Raymond et al. 2012) to estimate gas transfer velocities when obtaining field reaeration measurements is not feasible. However, large differences in flux estimations can be observed when calculating fluxes from both measured and modeled  $k$ . Differences were particularly evident at the quartz diorite site (RI), where average fluxes for all three gases were more than 57 times larger using modelled  $k$  than when using measured  $k$  (Table 2). These large differences in fluxes between the two methods of determining  $k$  are a result of the negative relationship between  $k$  and

discharge that was determined through field-based measurements of reaeration at RI. We trust this negative relationship because flow becomes more laminar and less turbulent during high discharge events at this site (RI), and it is common to observe decreases in  $k$  with increasing discharge (Aristegi et al. 2009). Although fluxes using modelled  $k$  were higher at RI and QP compared with measured  $k$ , they were lower at QS likely because of the steep stream slope at this site. Modelling approaches have been shown to be inadequate for turbulent streams with steep slopes (Hall Jr. and Madinger 2018), likely explaining the underestimation at QS. The field-based approach to determine  $k$  and ultimately calculate flux can account for geomorphological nuances that are missed using a modelling approach. Using the modelled approach alone in our study would have resulted in a significant overestimation of fluxes for all three GHGs at RI particularly. Future studies should consider whether there are unique geomorphological aspects of their study watersheds that could make modelled approaches less accurate.

In the Luquillo Mountains, stream CO<sub>2</sub> and N<sub>2</sub>O concentrations appear connected to terrestrial inputs, while CH<sub>4</sub> concentrations are driven by internal controls (i.e., O<sub>2</sub> availability and sediment characteristics). The lack of coherence surrounding controls and patterns among the three gases underscores the importance of considering the role of landscape heterogeneity. Whether or not our fluxes are higher or lower than other tropical streams varies among gases, challenging our ability to ascertain the role of tropical streams and rivers in fluvial emissions on a global scale. Increased direct, long-term, and high-quality greenhouse gas measurements and estimates of  $k$  from a more diverse range of tropical ecosystems are needed to further elucidate the drivers and fluxes of GHGs from fluvial tropical ecosystems, and ultimately to determine if the tropics are hotspots of emissions for all three gases.

**Acknowledgements** The data included in this paper would not be available without the work of field technicians including Brian Yudkin, Katherine Pérez Rivera, Kyle Zollo-Venecek, Tatiana Barreto Vélez, Jimmy Casey, Aneliya Cox, Alexis Sims, and Meaghan Shaw, and we acknowledge and thank them for their contributions. Support for this research was provided by National Science Foundation Long-Term Ecological Research 1831592, and National Science Foundation Critical Zone Observatory 1331841. Additional support was provided by the University of Puerto Rico and the USDA Forest Service

International Institute of Tropical Forestry. Partial funding was provided by the New Hampshire Agricultural Experiment Station. This is Scientific Contribution Number 2945. This work was supported by the United States Department of Agriculture National Institute of Food and Agriculture McIntire-Stennis Project 1019522.

**Author contributions** All authors contributed to the study conception and design. Data analysis was performed by AH and CLL with input from all authors. Flux calculations were performed by AH, JP, and CLL. The first draft of the manuscript was written by AH and all authors commented on previous versions of the manuscript and all authors read and approved the final manuscript.

**Funding** Support for this research was provided by National Science Foundation Long-Term Ecological Research 1831592, and National Science Foundation Critical Zone Observatory 1331841. Partial funding was provided by the New Hampshire Agricultural Experiment Station. This work was supported by the United States Department of Agriculture National Institute of Food and Agriculture McIntire-Stennis Project 1019522.

**Data availability** The datasets used for this study are available for public use: <http://www.hydroshare.org/resource/04f8de6f4da848218521291934f06eba>.

## Declarations

**Competing interests** The authors have no financial or non-financial interests to disclose.

## References

- Abrial G, Borges AV (2019) Ideas and perspectives: carbon leaks from flooded land: do we need to replumb the inland water active pipe? *Biogeosciences* 16:769–784. <https://doi.org/10.5194/bg-16-769-2019>
- Andrews LF, Wadnerkar PD, White SA et al (2021) Hydrological, geochemical and land use drivers of greenhouse gas dynamics in eleven sub-tropical streams. *Aquat Sci* 83:40. <https://doi.org/10.1007/s00027-021-00791-x>
- Aristegi L, Izagirre O, Elosegi A (2009) Comparison of several methods to calculate reaeration in streams, and their effects on estimation of metabolism. *Hydrobiologia* 635:113–124. <https://doi.org/10.1007/s10750-009-9904-8>
- Atkins ML, Santos IR, Maher DT (2017) Seasonal exports and drivers of dissolved inorganic and organic carbon, carbon dioxide, methane and δ13C signatures in a subtropical river network. *Sci Total Environ* 575:545–563. <https://doi.org/10.1016/j.scitotenv.2016.09.020>
- Audet J, Wallin MB, Kyllmar K et al (2017) Nitrous oxide emissions from streams in a Swedish agricultural catchment. *Agric Ecosyst Environ* 236:295–303. <https://doi.org/10.1016/j.agee.2016.12.012>
- Bange HW, Sim CH, Bastian D et al (2019) Nitrous oxide (N<sub>2</sub>O) and methane (CH<sub>4</sub>) in rivers and estuaries of

northwestern Borneo. *Biogeosciences* 16:4321–4335. <https://doi.org/10.5194/bg-16-4321-2019>

Barthel M, Bauters M, Baumgartner S et al (2022) Low N<sub>2</sub>O and variable CH<sub>4</sub> fluxes from tropical forest soils of the Congo Basin. *Nat Commun* 13:330. <https://doi.org/10.1038/s41467-022-27978-6>

Beaulieu JJ, Tank JL, Hamilton SK et al (2011) Nitrous oxide emission from denitrification in stream and river networks. *PNAS* 108:214–219. <https://doi.org/10.1073/pnas.1011464108>

Bodmer P, Wilkinson J, Lorde A (2020) Sediment properties drive spatial variability of potential methane production and oxidation in small streams. *J Geophys Res Biogeosci* 125:e2019JG005213. <https://doi.org/10.1029/2019JG005213>

Borges AV, Darchambeau F, Teodoro CR et al (2015) Globally significant greenhouse-gas emissions from African inland waters. *Nat Geosci* 8:637–642. <https://doi.org/10.1038/geo2486>

Burgin AJ, Hamilton SK (2007) Have we overemphasized the role of denitrification in aquatic ecosystems? A review of nitrate removal pathways. *Front Ecol Environ* 5:89–96

Cole JJ, Prairie YT, Caraco NF et al (2007) Plumbing the global carbon cycle: integrating inland waters into the terrestrial carbon budget. *Ecosystems* 10:172–185. <https://doi.org/10.1007/s10021-006-9013-8>

Crawford JT, Lottig NR, Stanley EH et al (2014) CO<sub>2</sub> and CH<sub>4</sub> emissions from streams in a lake-rich landscape: patterns, controls, and regional significance. *Glob Biogeochem Cycles* 28:197–210. <https://doi.org/10.1002/2013GB004661>

Drake TW, Raymond PA, Spencer RGM (2018) Terrestrial carbon inputs to inland waters: a current synthesis of estimates and uncertainty. *Limnol Oceanogr Lett* 3:132–142. <https://doi.org/10.1002/lo2.10055>

Duvert C, Bossa M, Tyler KJ et al (2019) Groundwater-derived DIC and carbonate buffering enhance fluvial CO<sub>2</sub> evasion in two Australian tropical rivers. *J Geophys Res Biogeosci* 124:312–327. <https://doi.org/10.1029/2018JG004912>

Hall RO Jr, Madinger HL (2018) Use of argon to measure gas exchange in turbulent mountain streams. *Biogeosciences* 15:3085–3092. <https://doi.org/10.5194/bg-15-3085-2018>

Herreid AM, Wymore AS, Varner RK et al (2020) Divergent controls on stream greenhouse gas concentrations across a land-use gradient. *Ecosystems*. <https://doi.org/10.1007/s10021-020-00584-7>

Hotchkiss ER, Hall RO Jr, Sponseller RA et al (2015) Sources of and processes controlling CO<sub>2</sub> emissions change with the size of streams and rivers. *Nat Geosci* 8:696–699. <https://doi.org/10.1038/geo2507>

Hynek SA, McDowell WH, Bhatt MP, Orlando JJ, Brantley SL (2022) Lithological control of stream chemistry in the Luquillo Mountains, Puerto Rico. *Front Earth Sci*. <https://doi.org/10.3389/feart.2022.779459>

Lauerwald R, Laruelle GG, Hartmann J et al (2015) Spatial patterns in CO<sub>2</sub> evasion from the global river network. *Glob Biogeochem Cycles* 29:534–554. <https://doi.org/10.1002/2014GB004941>

Liptzin D, Silver WL (2015) Spatial patterns in oxygen and redox sensitive biogeochemistry in tropical forest soils. *Ecosphere* 6:art211. <https://doi.org/10.1890/ES14-00309.1>

Liptzin D, Silver WL, Detto M (2011) Temporal dynamics in soil oxygen and greenhouse gases in two humid tropical forests. *Ecosystems* 14:171–182. <https://doi.org/10.1007/s10021-010-9402-x>

Marwick TR, Tamoh F, Ogwoka B et al (2018) A comprehensive biogeochemical record and annual flux estimates for the Sabaki River (Kenya). *Biogeosciences* 15:1683–1700. <https://doi.org/10.5194/bg-15-1683-2018>

McDowell WH, Bowden WB, Asbury CE (1992) Riparian nitrogen dynamics in two geomorphologically distinct tropical rain forest watersheds: subsurface solute patterns. *Biogeochemistry* 18:53–75. <https://doi.org/10.1007/BF00002703>

McDowell WH, Scatena FN, Waide RB et al (2012) Geographic and ecological setting of the Luquillo Mountains. Oxford University Press, Oxford

McDowell WH, Leon MC, Shattuck MD et al (2021) Luquillo experimental forest: catchment science in the montane tropics. *Hydro Process* 35:e14146. <https://doi.org/10.1002/hyp.14146>

Mulholland PJ, Valett HM, Webster JR et al (2004) Stream denitrification and total nitrate uptake rates measured using a field <sup>15</sup>N tracer addition approach. *Limnol Oceanogr* 49:809–820. <https://doi.org/10.4319/lo.2004.49.3.0809>

Murphy SF, Stallard RF, Scholl MA et al (2017) Reassessing rainfall in the Luquillo Mountains, Puerto Rico: local and global ecohydrological implications. *PLoS ONE* 12:e0180987. <https://doi.org/10.1371/journal.pone.0180987>

Oviedo-Vargas D, Genereux DP, Dierick D, Oberbauer SF (2015) The effect of regional groundwater on carbon dioxide and methane emissions from a lowland rainforest stream in Costa Rica. *J Geophys Res Biogeosci* 120:2579–2595. <https://doi.org/10.1002/2015JG003009>

Phillips CB, Jerolmack DJ (2016) Self-organization of river channels as a critical filter on climate signals. *Science* 352:694–697. <https://doi.org/10.1126/science.aad3348>

Pike AS, Scatena FN, Wohl EE (2010) Lithological and fluvial controls on the geomorphology of tropical montane stream channels in Puerto Rico. *Earth Surf Proc Land* 35:1402–1417. <https://doi.org/10.1002/esp.1978>

Potter JD, McDowell WH, Merriam JL et al (2010) Denitrification and total nitrate uptake in streams of a tropical landscape. *Ecol Appl* 20:2104–2115

Quick AM, Reeder WJ, Farrell TB et al (2019) Nitrous oxide from streams and rivers: a review of primary biogeochemical pathways and environmental variables. *Earth Sci Rev* 191:224–262. <https://doi.org/10.1016/j.earscirev.2019.02.021>

R Core Team (2021) R: a language and environment for statistical computing. R Foundation for Statistical Computing, Vienna, Austria. <https://www.R-project.org/>

Raymond PA, Zappa CJ, Butman D et al (2012) Scaling the gas transfer velocity and hydraulic geometry in streams and small rivers. *Limnol Oceanogr Fluids Environ* 2:41–53. <https://doi.org/10.1215/21573689-1597669>

Rocher-Ros G, Sponseller RA, Lidberg W et al (2019) Landscape process domains drive patterns of CO<sub>2</sub> evasion from

river networks. *Limnol Oceanogr Lett*. <https://doi.org/10.1002/lol2.10108>

Rodríguez-Cardona BM, Wymore AS, McDowell WH (2021) Nitrate uptake enhanced by availability of dissolved organic matter in tropical montane streams. *Freshw Sci* 40:65–76. <https://doi.org/10.1086/713070>

Rosentreter JA, Borges AV, Deemer BR, Holgerson MA et al (2021) Half of global methane emissions come from highly variable aquatic ecosystem sources. *Nat Geosci* 14:225–230. <https://doi.org/10.1038/s41561-021-00715-2>

Sadat-Noori M, Maher DT, Santos IR (2016) Groundwater discharge as a source of dissolved carbon and greenhouse gases in a subtropical estuary. *Estuaries Coasts* 39:639–656. <https://doi.org/10.1007/s12237-015-0042-4>

Sawakuchi HO, Bastviken D, Sawakuchi AO et al (2014) Methane emissions from Amazonian Rivers and their contribution to the global methane budget. *Glob Change Biol* 20:2829–2840. <https://doi.org/10.1111/gcb.12646>

Schneider CL, Herrera M, Raisle ML et al (2020) Carbon dioxide ( $\text{CO}_2$ ) fluxes from terrestrial and aquatic environments in a high-altitude tropical catchment. *J Geophys Res Biogeosci* 125:e2020JG005844. <https://doi.org/10.1029/2020JG005844>

Selvam BP, Natchimuthu S, Arunachalam L, Bastviken D (2014) Methane and carbon dioxide emissions from inland waters in India: implications for large scale greenhouse gas balances. *Glob Change Biol* 20:3397–3407. <https://doi.org/10.1111/gcb.12575>

Soued C, del Giorgio PA, Maranger R (2016) Nitrous oxide sinks and emissions in boreal aquatic networks in Québec. *Nat Geosci* 9:116–120. <https://doi.org/10.1038/ngeo2611>

Stanley EH, Casson NJ, Christel ST et al (2016) The ecology of methane in streams and rivers: patterns, controls, and global significance. *Ecol Monogr* 86:146–171. <https://doi.org/10.1890/15-1027>

Teodoru CR, Nyoni FC, Borges AV, Darchambeau F, Nyambe I, Bouillon S (2015) Dynamics of greenhouse gases ( $\text{CO}_2$ ,  $\text{CH}_4$ ,  $\text{N}_2\text{O}$ ) along the Zambezi River and major tributaries, and their importance in the riverine carbon budget. *Biogeosciences* 12:2431–2453. <https://doi.org/10.5194/bg-12-2431-2015>

Ulseth AJ, Hall RO Jr, Canadell MB, Madinger HL, Niayifar A, Battin TJ (2019) Distinct air-water gas exchange regimes in low- and high-energy streams. *Nat Geosci* 12:259–263. <https://doi.org/10.1038/s41561-019-0324-8>

Upstill-Goddard RC, Salter ME, Mann PJ et al (2017) The riverine source of  $\text{CH}_4$  and  $\text{N}_2\text{O}$  from the Republic of Congo, western Congo Basin. *Biogeosciences* 14:2267–2281. <https://doi.org/10.5194/bg-14-2267-2017>

Wanninkhof R, Mulholland PJ, Elwood JW (1990) Gas exchange rates for a first-order stream determined with deliberate and natural tracers. *Water Resour Res* 26:1621–1630. <https://doi.org/10.1029/WR026i007p01621>

Wymore AS, Brereton RL, Ibarra DE, Maher K, McDowell WH (2017) Critical zone structure controls concentration-discharge relationships and solute generation in forested tropical montane watersheds. *Water Resour Res* 53:6279–6295. <https://doi.org/10.1002/2016WR020016>

Wymore AS, Leon MC, Shanley JB, McDowell WH (2019) Hysteretic response of solutes and turbidity at the event scale across forested tropical montane watersheds. *Front Earth Sci*. <https://doi.org/10.3389/feart.2019.00126>

Zheng Y, Wu S, Xiao S, Yu K, Fang X, Xia L, Wang J, Liu S, Freeman C, Zou J (2022) Global methane and nitrous oxide emissions from inland waters and estuaries. *Glob Change Biol* 28:4713–4725. <https://doi.org/10.1111/gcb.16233>

**Publisher's Note** Springer Nature remains neutral with regard to jurisdictional claims in published maps and institutional affiliations.

Springer Nature or its licensor (e.g. a society or other partner) holds exclusive rights to this article under a publishing agreement with the author(s) or other rightsholder(s); author self-archiving of the accepted manuscript version of this article is solely governed by the terms of such publishing agreement and applicable law.